FULL PAPER

Dalton
www.rsc.org/dalton

A solid-state study of eight-coordinate lanthanide(III) complexes (Ln = Eu, Gd, Tb, Dy) with 1-hydroxy-2-pyridinone

Christine Tedeschi,[a] Joëlle Azéma,[a] Heinz Gornitzka,[b] Pierre Tisnès[a] and Claude Picard *[a]
[a] *Laboratoire de Synthèse et Physicochimie de Molécules d'Intérêt Biologique, CNRS UMR 5068, Université Paul Sabatier, 118 route de Narbonne, 31062 Toulouse cedex 04, France. E-mail: picard@chimie.ups-tlse.fr*
[b] *Laboratoire d'Hétérochimie Fondamentale et Appliquée, CNRS UMR 5069, Université Paul Sabatier, 118 route de Narbonne, 31062 Toulouse cedex 04, France*

Received 6th January 2003, Accepted 7th March 2003
First published as an Advance Article on the web 20th March 2003

Four lanthanide complexes of 1-hydroxy-2-pyridinone (HOPO) have been synthesised from aqueous solution at pH ≈ 7 and their structures and luminescent properties have been established. This ligand coordinates to lanthanide(III) ions as an anionic bidentate chelate (1-oxy-2-pyridinonate, OPO^-) and crystallographic analyses show the formation of two structural types with different stoichiometries. In the first part of this series (Eu, Gd) the structural type consists of dimer units $Na_2[Ln_2(OPO)_8]\cdot 9H_2O$, crystallising in the orthorhombic system, space group $P2_12_12_1$. The immediate coordination sphere around Ln is occupied by the eight oxygen atoms of four bidentate OPO^- ligands. These complexes display the Na^+ ions associated with the complex anion *via* interactions with bridging CO and NO groups of the ligands, inducing a polymeric structure. In the second part of the series (Tb, Dy) the structures obtained are $[Ln(OPO)_3(H_2O)_2]\cdot H_2O$, crystallising in triclinic system, space group $P\bar{1}$. The Tb(III) and Dy(III) ions are also eight-coordinated but two water molecules occupy the coordination sphere instead of one ligand OPO^-. The Dy(III), Eu(III) and Tb(III) complexes display in the solid state and at room temperature a photoluminescence that is achieved by an indirect excitation process (antenna effect). The terbium(III) complex exhibits intense sensitized green emission, which is temperature independent.

Introduction

Although the 4f block ions display mainly the same formal charge (3+) and similar chemical properties, their coordination chemistry has become of increasing significance in the last few years. This is due to their electronic, magnetic and spectroscopic properties, which are different along the complete series and may widely be applied in various fields.[1] As far as biomedical fields are concerned, the fast developing applications of lanthanide containing systems in magnetic resonance imaging,[2] cancer diagnostic,[3] therapy,[4] time-resolved fluoroimmunoassays,[5] luminescent labelling of biomolecules in the visible,[6] and near-IR[7] spectral domains are relevant examples of this renewed interest.

Ln(III) ions behave as hard acids with a strong affinity for hard bases like neutral and negatively charged oxygen atoms. As a consequence, β-diketones which act as bidentate units, and other negatively charged {O,O} donors are widely used as ligands in lanthanide coordination chemistry.[8] Unidentate groups such as carboxylate, phosphate and phosphinate are other examples of binding units incorporated in lanthanide chelates of practical use.[9] On the other hand, hydroxamic acids [CO–N(R)OH] are versatile chelating agents able to effectively bind a variety of metal ions.[10] In most metal complexes found with these ligands, the deprotonated hydroxyl group and carbonyl oxygen are involved in the coordination to the metal ion. Thus, the hydroxamate functional group behaves as a typical bidentate {O,O} ligand, forming energetically-favourable five-membered chelate rings. The chemistry of transition metal hydroxamates has attracted considerable attention because of their bioorganic relevance. Particularly hydroxamic acids are intimately associated with the bacterial iron transport mechanism in the life process.[11] They have also been used extensively as organic extractants capable of removal of actinides from aqueous process waste streams.[12] In contrast, there have been very few reports on the interaction of hydroxamates with lanthanide ions, in spite of the high affinity of these binding units towards Ln(III). Martell and co-workers[13] have investigated the lanthanide chelating ability in aqueous solutions of several hydroxamic acids and reported high stability constants in this solvent for Ln–trihydroxamato complexes ($\log\beta_{ML} = 18$, M = Yb, L = BAMTPH, a synthetic trihydroxamic acid). On the other hand, Chatterjee[10] briefly reviewed the lanthanide hydroxamate complexes derived from simple hydroxamic acids. With these ligands, the lanthanide complexes were found as mononuclear ML_3 species. These structures were supported by elemental analytical data but have not been structurally evidenced by X-ray crystallography. More structural data are available on the interaction of lanthanide with amino derivatives of hydroxamic acids.[14] Very recently, an X-ray analysis of DL-α-alaninehydroxamic acid with Eu(III) has shown the existence of a binuclear complex, $[Eu(DL\text{-}\alpha\text{-}Alaha)(H_2O)_6]_2(ClO_4)_6$. In this complex, CO and NOH groups are involved in metal binding and the NO group acts as an additional bridging role, forming binuclear systems.[15]

In this context and in connection with our interest in the photophysics of lanthanide complexes,[16] we were interested in studying the structures and properties of luminescent lanthanide complexes with the 1-hydroxy-2-pyridinone ligand (Scheme 1). This moiety can be thought of as a cyclic hydroxamic acid and data obtained by UV, IR, NMR spectroscopy and X-ray crystallography support this representation.[17,18] Moreover this aromatic structure can act as a sensitizer for the lanthanide-centred luminescence by energy transfer from a ligand-centred excited state (antenna effect).[19,20] In this paper, we report the syntheses and crystal structures of the tetrakis complexes of 1-hydroxy-2-pyridinonate (OPO^-) with Eu(III) and Gd(III), the syntheses and the structures of the tris

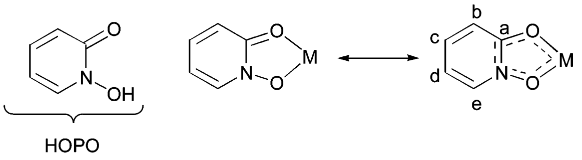

Scheme 1

DOI: 10.1039/b300159h

(OPO^-) complexes of Tb(III) and Dy(III), and discuss their luminescent properties in the solid state. To the best of our knowledge, no lanthanide crystal structure of Ln^{3+} complexes derived from an aromatic hydroxamate ligand has been reported until now. In addition, these ligands have not been previously used to sensitize Ln^{3+} emission. Preliminary results for the Tb^{3+} complex have been published.[21]

Experimental

Chemicals

1-Hydroxy-2-pyridinone (2-hydroxypyridine *N*-oxide) was purchased from Aldrich and was purified as follows. A 20 wt% solution of HOPO ligand in water was acidified to pH 1 with 1 M HCl and extracted with ethyl acetate. The extract was dried over Na_2SO_4, the solvent was evaporated and the solid residue was sublimed (120 °C/0.13 mbar). Mp 148–149 °C (lit.,[22] 149–150 °C).

Lanthanide chloride salts were purchased from Aldrich ($GdCl_3\cdot6H_2O$, $TbCl_3\cdot6H_2O$), Strem Chemicals ($EuCl_3\cdot6H_2O$), and Avocado Research Chemical ($DyCl_3\cdot6H_2O$) and were used without further purification.

Physical measurements

Microanalyses (C, H, N) were carried out by the "Service Commun de Microanalyse élémentaire UPS-INP" in Toulouse. Infrared spectra were obtained from KBr pellets with a Perkin-Elmer spectrometer. The electrospray ionisation mass spectra were recorded on a Perkin-Elmer SCIEX API spectrometer in methanol solution. Phosphorescence spectra and lifetimes were obtained with a LS-50B Perkin-Elmer spectrofluorimeter equipped with a Hamamatsu R928 photomultiplier tube and the low-temperature accessory No L2250136. Solid state samples were finely powdered and dispersed in a KBr matrix. The excitation spectra were automatically corrected, and the emission spectra were corrected according to the instrument guidebook. Lifetimes τ (uncertainty $\leq$5%) are the average values from at least five separate measurements which were made by monitoring the decay at a wavelength corresponding to the maximum intensity of the emission spectrum, following pulsed excitation. The phosphorescence decay curves were fitted by an equation of the form $I(t) = I(0)\exp(-t/\tau)$ using a curve-fitting program. The high-resolution emission spectrum of the europium complex was registered on a Dilor XY dispersive spectrometer equipped with a Thomson 1024 CCD detector. The exciting source is a krypton-argon ion laser; the 488 nm line was selected.

Preparation of complexes

The metal complexes were prepared as follows: 366 mg (3.3 mmol) of HOPO ligand were dissolved in 200 mL of distilled water and the pH was adjusted to 7.0 with 0.5 M NaOH. To this stirred solution was added dropwise $LnCl_3\cdot6H_2O$ (1 mmol) in distilled water (2 mL), at room temperature. Upon slow evaporation of the water (several days), colorless crystals of suitable quality for X-ray crystallographic analysis were obtained. No precaution was taken against the access of air, since the complexes are sufficiently stable.

Analysis for $Na[Eu(OPO)_4]\cdot4.5H_2O$ (1). Found: C, 34.71; H, 3.04; N, 7.97. $C_{20}H_{25}N_4O_{12.5}EuNa$ requires C, 34.50; H, 3.62; N, 8.05%. Selected IR bands: $\tilde{\nu}$/cm^{-1} 3392 (br), 3260 (sh), 3092w, 1621s, 1525s, 1449w, 1372s, 1187s, 1150m, 1117m, 1033w, 934w, 887m, 852w, 789m, 751m, 602m, 551w, 461w. ESI$^+$-MS: *m*/*z* 987.1 ($[Eu_2(OPO)_6Na]^+$, 44%), 854.1 ($[Eu_2(OPO)_5]^+$, 20%), 639.1 ($[Eu(OPO)_4Na_2]^+$, 44%), 506.0 ($[Eu(OPO)_3Na]^+$, 100%). ESI$^-$-MS: *m*/*z* 994.9 ($[Eu_2(OPO)_6(OCH_3)]^-$, 10%), 592.9 ($[Eu(OPO)_4]^-$, 100%), 514.0 ($[Eu(OPO)_3(OCH_3)]^-$, 31%), 482.9 ($[Eu(OPO)_3]^-$, 19%). Luminescence (295 K, λ_{exc} 320 nm): λ_{em}/nm 582 (relative intensity, 0.8), 596 (5.2), 614 (100), 653 (4.1), 695 (2.8), 708 (6.1).

Analysis for $Na[Gd(OPO)_4]\cdot4.5H_2O$ (2). Found: C, 33.58; H, 3.37; N, 7.65. $C_{20}H_{25}N_4O_{12.5}GdNa$ requires C, 34.24; H, 3.59; N, 7.98%. Selected IR bands: $\tilde{\nu}$/cm^{-1} 3400 (br), 3260 (br), 3090w, 1621s, 1525s, 1449w, 1372s, 1190s, 1152m, 1118m, 1032w, 945 w, 887m, 850w, 790m, 749m, 602m, 550w, 466w. Luminescence (77 K, λ_{exc} 320 nm): λ_{em}/nm 499.

Analysis for $[Tb(OPO)_3(H_2O)_2]\cdot H_2O$ (3). Found: C, 33.25; H, 3.17; N, 7.64. $C_{15}H_{18}N_3O_9Tb$ requires C, 33.16; H, 3.34; N, 7.73%. Selected IR bands: $\tilde{\nu}$/cm^{-1}) 3420 (br), 3250 (br), 3090w, 1621s, 1526s, 1449w, 1372s, 1189s, 1151m, 1118m, 1033w, 934w, 888m, 850w, 790 m, 751m, 602m, 551w, 466w. ESI$^+$-MS: *m*/*z* 1001.0 ($[Tb_2(OPO)_6Na]^+$, 81%), 868.1 ($[Tb_2(OPO)_5]^+$, 75%), 645.0 ($[Tb(OPO)_4Na_2]^+$, 11%), 512.1 ($[Tb(OPO)_3Na]^+$, 100%). Luminescence (295 K, λ_{exc} 320 nm): λ_{em}/nm 489 (relative intensity, 23.1), 547 (100), 588 (13.4), 622 (11.6).

Analysis for $[Dy(OPO)_3(H_2O)_2]\cdot H_2O$ (4). Found: C, 33.25; H, 3.20; N, 7.62. $C_{15}H_{18}N_3O_9Dy$ requires C, 32.95; H, 3.32; N, 7.68%. Selected IR bands: $\tilde{\nu}$/cm^{-1} 3430 (br), 3270 (br), 3068w, 1623s, 1526s, 1449w, 1373s, 1196s, 1159m, 1118m, 1031w, 949w, 887m, 840w, 791 m, 778w, 745m, 603m, 546w, 471w. Luminescence (295 K, λ_{exc} 320 nm): λ_{em}/nm 484 (relative intensity, 26.5), 579 (100), 663 (8.7), 755 (8.1).

Crystallography

A summary of the crystal data and of the data collection and refinement parameters for complexes **1**,**2** and **4** is given in Table 1.

Data for all structures were collected at low temperatures using an oil-coated shock-cooled crystal on a Bruker-AXS CCD 1000 diffractometer with Mo-Kα radiation (λ = 0.71073 Å). The structures were solved by direct methods (SHELXS-97) [23] and all non hydrogen atoms were refined anisotropically using the least-squares method on F^2.[24]

CCDC reference numbers 200686–200688.

See http://www.rsc.org/suppdata/dt/b3/b300159h/ for crystallographic data in CIF or other electronic format.

The crystal structure of the Tb(III) complex **3** was reported in a preliminary communication.[21] CCDC reference number 440/199. See http://www.rsc.org/suppdata/nj/b0/b004288i/ for crystallographic data in CIF or other electronic format.

Results and discussion

Preparation and characterisation of the complexes

In papers dealing with lanthanide complexes of simple hydroxamic acids and lanthanide ions,[10,25,26] IR data and elemental analyses support the existence of LnL_3 complexes containing deprotonated hydroxamic acid as a binucleating ligand with the carbonyl and hydroximate oxygens bound to metal. Consequently, we studied the coordination chemistry of HOPO ligand with lanthanide(III) salts (Eu, Gd, Tb, Dy) using ligand : metal ratio of 3 : 1 and we focused our attention on the isolation of crystalline products suitable for full X-ray structural characterisation. The initial reactions explored were those with lanthanide carbonate.[27] Despite variation in several synthetic parameters, *e.g.* solvent and temperature, we could isolate only powders with poor crystallinity. The 3 : 1 reactions between HOPO and lanthanide chlorides in aqueous solution (pH 7) resulted in the slow formation of a crystalline material in each case. These complexes exhibit good stability with respect to the atmosphere over a long time scale.

The general pattern of the infrared spectra of all the complexes supports the normal coordination of the hydroxamic

Table 1 Crystal data and structure refinement for complexes **1**, **2** and **4**.

	1	**2**	**4**
Empirical formula	$C_{40}H_{50}N_8O_{25}Na_2Eu_2$	$C_{20}H_{25}N_4O_{12.5}NaGd$	$C_{15}H_{18}N_3O_9Dy$
Formula weight	1392.78	701.68	546.82
Crystal system	Orthorhombic	Orthorhombic	Triclinic
Space group	$P2_12_12_1$	$P2_12_12_1$	$P\bar{1}$
a/Å	14.1076(5)	14.1145(6)	6.3254(2)
b/Å	19.1111(7)	19.1011(7)	11.7520(4)
c/Å	19.2936(7)	19.2734(7)	13.6109(5)
α/°	90	90	103.706(1)
β/°	90	90	100.737(1)
γ/°	90	90	104.508(1)
V/Å^3	5201.8(3)	5196.2(3)	918.59(5)
Z	4	8	2
D_c/Mg m^{-3}	1.778	1.794	1.977
T/K	193(2)	193(2)	193(2)
μ/mm^{-1}	2.499	2.640	4.123
R_{int}	0.0582	0.0397	0.0193
2θ max/°	66	56	64
Reflns. measured	71439	38047	15602
Reflns. independent	19598	12904	6182
Parameters	748	748	277
Final R [$I > 2\sigma(I)$]	0.0315	0.0316	0.0175
$wR2$ (all data)	0.0713	0.0626	0.0453
Goodness of fit on F^2	1.023	0.962	1.022

group *via* the ketonic oxygen atom and the oxygen atom of the deprotonated NO$^-$ group. These data were obtained by recording IR spectra of the ligand and isolated lanthanide complexes in KBr pellets. The intermolecular H-bonded OH stretching vibration of HOPO is assigned in the region of 2500 cm^{-1}. This broad band disappears in the lanthanide complexes, indicating a complete deprotonation of the N–OH group. On the other hand, new bands in the spectra of metal complexes occurring at *ca* 3400 and 3200 cm^{-1} are due to the lattice and coordinated water molecules. All lanthanide complexes exhibit for $\nu_{C=O}$ a decrease of the carbonyl stretching vibration frequency relative to that of the free ligand ($\Delta\tilde{\nu}$ ~ 15 cm^{-1}). This red shift is underestimated, if we consider the existence, in the solid state, of intermolecular hydrogen bonds in the free ligand.[18] When IR spectrum of HOPO in solution (chloroform) is taken as a reference, larger shifts are calculated (~32 cm^{-1}). A variation of the same amplitude was reported by Agrawal and Shukla for lanthanide complexes with *N*-phenylbenzohydroxamic acids.[25] This is due to a decrease of the double bond character of the C=O bond due to the participation of the oxygen atom of carbonyl groups in the complexation. On the other hand, the ring-stretching modes (1530–1370 cm^{-1}) are almost unaffected in the lanthanide complexes. As far as the vibration associated with the N–O group is concerned, it generally appears at 1250–900 cm^{-1} in metal hydroxamate complexes.[26,28] A strong band occurs in the four lanthanide complexes at *ca.* 1190 cm^{-1}, which can be assigned qualitatively to the NO stretching vibration. The frequency is similar to those for ν(NO) bands in complexes Cu(OPO)$_2$ and Fe(OPO)$_3$-H$_2$O.[29] Katritzky and Jones[30] assigned ν(NO) at 1110 cm^{-1} for the free ligand in chloroform solution (1115 cm^{-1} in KBr disk). The observed blue shift is attributable to the resonance in the coordinated hydroxamate ligand. The NO group is strengthened by equalisation of single–double bond length upon lanthanide complexation, leading to an increase in vibrational frequency. This result is in concordance with the crystal structure analyses (*vide infra*) in which the average bond length of the NO group in lanthanide complexes is shorter than that in the free ligand (1.32 Å *vs.* 1.38 Å).

As far as the ligand : metal stoichiometry is concerned, elemental analytical data (C, H, N) are consistent with the formation of 3 : 1 complexes corresponding to the formulation [Ln(OPO)$_3$·nH$_2$O] (n = 2 or 3). However, calculations with a 4 : 1 ligand : metal ratio corresponding to the formulation [Na Ln(OPO)$_4$·nH$_2$O] (n = 4.5 or 5) are not too far off the experimental values. Although electrospray ionisation mass spectrometry (ESIMS) is used to establish the nature of lanthanide complexes,[31] ESIMS experiments conducted on europium and terbium complexes, **1** and **3**, give no precise information about their stoichiometry. The negative-ion ESI mass spectrum of the europium complex in methanol shows [Eu(OPO)$_3$(OCH$_3$)]$^-$ and [Eu(OPO)$_4$]$^-$ species as the main anions in the gas phase. The positive ionisation spectrum gives a relatively intense peak at *m*/*z* 639.1 due to the ion [Eu(OPO)$_4$Na$_2$]$^+$, but is dominated by the peak at *m*/*z* 506.0, corresponding to the ion [Eu(OPO)$_3$Na]$^+$. In the terbium complex, [Tb(OPO)$_3$Na]$^+$ is the base peak, but higher mass ions [Tb$_x$(OPO)$_y$Na$_{y+1-3x}$]$^+$ are also observed. These diverse ionic species can be accounted for in terms of fragmentation, ligand exchange and clustering reactions. Such reactions are also observed in the ESI-mass spectra of lanthanide β-diketone complexes.[32] Although, the analysis of sodium ion would provide an answer in distinguishing the two potential classes of these complexes, the availability of good quality crystals has allowed us to establish unambiguously their structures. The single-crystal X-ray study (*vide infra*) shows that the ligand : metal stoichiometry of the products obtained depends on the position of the metal ion in the lanthanide series. The reaction of the lanthanides with HOPO ligand in a 3 : 1 ligand : metal ratio results in the formation of ML$_4$ (M = Eu, Gd) and ML$_3$ (M = Tb, Dy) complexes. Such change in stoichiometry, which is often correlated with the size of the ion, is a well-established feature of lanthanide chemistry. The transition point occurring at gadolinium was reported before for other bidentate ligands.[33]

Crystal structures

The X-ray structure data for complex **1** shows that the unit cell contains one tetranuclear sub-unit with two europium centres which are each eight-coordinated by four ligands OPO$^-$. Thus, compound **1** is ionic and consists of the complex anions [Eu (OPO)$_4$]$^-$, counter ions (Na$^+$) and nine water molecules. The molecular structure of **1** and the numbering scheme is shown in Fig. 1, and selected bond lengths and angles are listed in Table 2. The deprotonated OPO ligand is coordinated to europium ion as a bidentate {O,O} donor forming five-membered chelate rings with a bite angle of ~65.5°. The Eu(III) ion has a structure with no crystallographically imposed symmetry. The average Eu–O$_N$ distance, 2.394 Å (range 2.405–2.381 Å) is similar to the average Eu–O$_C$ distance, 2.391 Å

Table 2 Selected bond lengths (Å) and angles (°) for complexes **1** (Ln = Eu) and **2** (Ln = Gd)

Complex **1**				Complex **2**			
Eu(1)–Eu(2)	7.046	O(1)–Eu(1)–O(2)	65.41(7)	Gd(1)–Gd(2)	7.045	O(1)–Gd(1)–O(2)	65.76(12)
Eu(1)–O(1)	2.395(2)	O(3)–Eu(1)–O(4)	66.04(7)	Gd(1)–O(1)	2.386(3)	O(3)–Gd(1)–O(4)	66.79(11)
Eu(1)–O(2)	2.406(2)	O(5)–Eu(1)–O(6)	65.66(7)	Gd(1)–O(2)	2.405(3)	O(5)–Gd(1)–O(6)	66.11(12)
Eu(1)–O(3)	2.369(2)	O(7)–Eu(1)–O(8)	65.86(7)	Gd(1)–O(3)	2.350(4)	O(7)–Gd(1)–O(8)	66.25(13)
Eu(1)–O(4)	2.404(2)	O(9)–Eu(2)–O(10)	65.11(7)	Gd(1)–O(4)	2.383(4)	O(9)–Gd(2)–O(10)	65.54(12)
Eu(1)–O(5)	2.401(2)	O(11)–Eu(2)–O(12)	65.76(7)	Gd(1)–O(5)	2.397(3)	O(11)–Gd(2)–O(12)	66.00(11)
Eu(1)–O(6)	2.390(2)	O(13)–Eu(2)–O(14)	65.48(7)	Gd(1)–O(6)	2.381(3)	O(13)–Gd(2)–O(14)	65.87(11)
Eu(1)–O(7)	2.390(2)	O(15)–Eu(2)–O(16)	65.98(7)	Gd(1)–O(7)	2.383(3)	O(15)–Gd(2)–O(16)	66.05(12)
Eu(1)–O(8)	2.390(2)	Eu(1)–O(2)–C(1)	119.92(17)	Gd(1)–O(8)	2.383(3)	Gd(1)–O(2)–C(1)	119.60(3)
Eu(2)–O(9)	2.390(2)	O(2)–C(1)–N(1)	118.00(2)	Gd(2)–O(9)	2.377(3)	O(2)–C(1)–N(1)	118.50(5)
Eu(2)–O(10)	2.413(2)	C(1)–N(1)–O(1)	117.40(2)	Gd(2)–O(10)	2.400(4)	C(1)–N(1)–O(1)	117.10(4)
Eu(2)–O(11)	2.381(2)	N(1)–O(1)–Eu(1)	118.57(15)	Gd(2)–O(11)	2.368(3)	N(1)–O(1)–Gd(1)	118.20(3)
Eu(2)–O(12)	2.388(2)	Eu(2)–O(10)–C(21)	119.21(17)	Gd(2)–O(12)	2.375(3)	Gd(2)–O(10)–C(21)	119.10(3)
Eu(2)–O(13)	2.388(2)	O(10)–C(21)–N(5)	117.30(2)	Gd(2)–O(13)	2.375(3)	O(10)–C(21)–N(5)	117.20(4)
Eu(2)–O(14)	2.405(2)	C(21)–N(5)–O(9)	118.00(2)	Gd(2)–O(14)	2.390(3)	C(21)–N(5)–O(9)	118.50(4)
Eu(2)–O(15)	2.370(2)	N(5)–O(9)–Eu(2)	119.63(16)	Gd(2)–O(15)	2.379(3)	N(5)–O(9)–Gd(2)	118.80(3)
Eu(2)–O(16)	2.396(2)			Gd(2)–O(16)	2.401(3)		

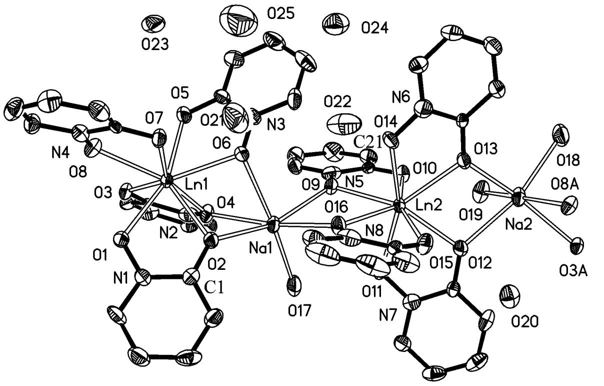

Fig. 1 View of the dimer unit and the coordination environment around the Ln(III) ions in compounds **1** (Ln = Eu) and **2** (Ln = Gd) with the atom numbering scheme. Hydrogen atoms are omitted for simplicity.

(range 2.413–2.370 Å), indicating that the OPO ligands are symmetrically bonded to Eu(III). Using Shannon's definition[34] (with r_O = 1.31 Å), and by taking into account the eight contacts, we calculate an effective ionic radius for Eu(III) of 1.08 Å, in agreement with the reported value for eight-coordinate Eu(III) complexes (1.066 Å).[35] The anionic complex units are held together in the crystals *via* sodium cations leading to a ionically linked polymeric chain (Fig. 2) that extends in the crystal. The linking sodium cations present two coordination spheres. Na(1) forms five interactions to two anionic complex units involving four NO oxygen atoms and one carbonyl oxygen [O(4), O(6), O(9), O(16) and O(2) respectively]. The immediate Na(1) coordination sphere is completed by an aqua ligand [O(17)]. Na(2) interacts with two water molecules [O(18), O(19)], three carbonyl oxygens [O(12), O(13), O(3A)] and one NO oxygen [O(8A)]. The two sodium ions are therefore six-coordinated with Na–O distances in the range of 2.360–2.462 Å, which are normal for sodium cations.[36] The oxygen atoms of the OPO^- ligand are bridging between the lanthanide ion and the Na^+ ion. Consequently, in compound **1**, this ligand exhibits three binding modes. One OPO^- ligand uses its two oxygen atoms as monoatomic bridges linking the lanthanide and sodium ions. The remaining OPO^- ligands are bound by using the deprotonated hydroxyl oxygen or the carbonyl oxygen as bridging atoms. As far as the lanthanide complexes are concerned, a NO function of a hydroxamic ligand bridging two metal centres has been reported by Galdecka *et al.*[15] On the other hand, a monoatomic bridge linking a lanthanide ion (Pr(III), Nd(III)) and a sodium ion has been very recently observed for the oxygen atoms of an oxamido ligand (1,4,8,11-tetraazacyclotetradecane-2,3-dione).[37] The complex anions are also held together by hydrogen bonds involving water molecules coordinated to sodium ions. For example, O(19) attached to Na(2) is hydrogen bonded to the ligand amide oxygen O(10) of one complex anion, while the second aqua ligand O(18) is hydrogen bonded to the ligand amide oxygen (O5A) of another complex anion (non-bonded O ··· O separations 2.783 and 2.715 Å, respectively. We also notice an extensive hydrogen bonding between five lattice water molecules [O(21), O(22), O(23), O(24) and O(25)]. On the other hand, it is well known that O–H oscillators (water molecules) are the most effective quenchers of the Eu(III) luminescence both in solution and in the solid state.[38] These O–H groups act independently, but the sensitivity of the rate of quenching decreases as the distance between the lanthanide ion and a proximate oscillator increases. In the crystal lattice of compound **1**, the nearest water molecules are those bound to the Na^+ ion [Eu(2)–O(19): 4.156 Å, Eu(1)–O(18): 4.202 Å]. The nearest lattice water is 4.431 Å [Eu(1)–O(21)] away from the eight-coordinate europium ion. Metal–metal separations are also significant with regard to electronic interactions affecting luminescence behaviour;[39] the shortest Eu ··· Na separation is 3.497 Å, while the Eu ··· Eu separation is 7.046 Å across the linking Na^+ centres.

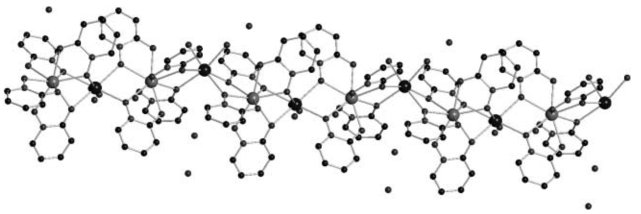

Fig. 2 View of the polymeric chain in the structure of compounds **1** and **2**.

The structure of compound **2** is similar to that of **1** and consists of tetranuclear $[Na_2Gd_2(OPO)_4(H_2O)_3]\cdot 6H_2O$ units. The numbering scheme of **2** is the same as for **1**; selected bond lengths and angles are presented in Table 2. The gadolinium ion has a eight-coordinate inner sphere environment composed of the oxygen atoms from four bidentate OPO^- ligands (bite angle of ~ 66°). The Gd–O bonds involving the ligand donor atoms are similar to compound **1**: average Gd–O_N distance 2.384 Å, average Gd–O_C distance 2.383 Å. The sodium ion links two complex anions (shortest Gd–Na distance 3.492 Å) *via* bridging oxygen atoms of the hydroxamic acid molecules as mentioned above. As in the case of compound **1**, six lattice water are present in the unit cell.

The X-ray study of **3**[21] and **4** reveals that these compounds are isostructural and have a more simple structure than the relatively complex one found for **1** and **2**. In complexes **3** and **4**, the structure determination confirms the 3 : 1 ligand : metal stoichiometry and shows that the Ln(III) centre (Ln = Tb, Dy) is

Table 3 Selected bond lengths (Å) and angles (°) for complexes **3**[21] (Ln = Tb) and **4** (Ln = Dy)

Complex **3**				Complex **4**			
Tb–O(1)	2.411(2)	O(1)–Tb–O(2)	65.50(8)	Dy–O(1)	2.404(12)	O(1)–Dy–O(2)	65.79(5)
Tb–O(2)	2.315(2)	O(3)–Tb–O(4)	65.55(8)	Dy–O(2)	2.311(14)	O(3)–Dy–O(4)	65.87(4)
Tb–O(3)	2.368(2)	O(5)–Tb–O(6)	65.87(8)	Dy–O(3)	2.366(12)	O(5)–Dy–O(6)	66.25(4)
Tb–O(4)	2.376(2)	O(7)–Tb–O(8)	72.20(11)	Dy–O(4)	2.369(13)	O(7)–Dy–O(8)	72.11(5)
Tb–O(5)	2.366(2)	Tb–O(2)–C(1)	121.70(2)	Dy–O(5)	2.365(12)	Dy–O(2)–C(1)	121.82(11)
Tb–O(6)	2.370(2)	O(2)–C(1)–N(1)	117.20(3)	Dy–O(6)	2.368(12)	O(2)–C(1)–N(1)	117.25(15)
Tb–O(7)	2.350(3)	C(1)–N(1)–O(1)	116.90(3)	Dy–O(7)	2.348(13)	C(1)–N(1)–O(1)	116.44(14)
Tb–O(8)	2.434(3)	N(1)–O(1)–Tb	118.04(19)	Dy–O(8)	2.427(15)	N(1)–O(1)–Dy	118.11(10)

eight-coordinated by three bidentate ligands OPO^- and two water molecules. A third water molecule is also found in the second coordination sphere of Ln(III). Fig. 3 shows a perspective view of the $[Ln(OPO)_3(H_2O)_2]\cdot H_2O$ unit with atom numbering. Selected bond distances and angles are listed in Table 3. The shortest lanthanide to ligand bond length is to the oxygen of a CO group [Tb–O(2) 2.315 Å, Dy–O(2) 2.311 Å], the longest is to a water group [Tb–O(8) 2.434 Å, Dy–O(8) 2.427 Å]. Two of the OPO ligands are symmetrically chelated to the lanthanide ion (average bond distance 2.370 Å), while the third is asymmetric with the $Ln–O_N$ bond being longer than the $Ln–O_C$ bond [Tb–O(1) 2.411 and Tb–O(2) 2.315 Å, Dy–O(1) 2.404 and Dy–O(2) 2.311 Å]. This probably results from optimisation of the ligand arrangements in the inner sphere. It is worth noting that the average Tb–O(OPO) bond distance in **3** is close to that found in structures of β-diketonate complexes of terbium. For example, a eight-coordinate complex with three hexafluoroacetylacetone ligands and two water molecules has Tb–O(hfa) distances in the range 2.321–2.401 Å.[40] In **3** and **4** the coordinated water molecules O(7) and O(8) are at 2.35 and 2.43 Å from the lanthanide, respectively. The last value falls within the range of metal–H_2O distances observed in other eight-coordinate lanthanide complexes containing water molecules in the first coordination sphere of the metal, while the first value is indicative of a rather strong bond and is slightly shorter than the average Ln–O(OPO) distance. The third water molecule O(9) involved in each molecular unit is not bonded to the metal (the Ln–O(9) distance is ~4.52 Å), but is connected to the complex molecule *via* hydrogen bonding with oxypyridinone moiety.

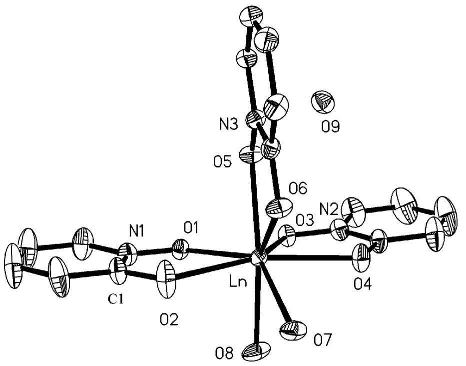

Fig. 3 View of the coordination environment around the Ln(III) atom in the structure of compounds **3**[21] (Ln = Tb) and **4** (Ln = Dy) with the atom numbering scheme. Hydrogen atoms are omitted for simplicity.

Table 4 shows average bond lengths in complexes **1**–**4**, as well as the corresponding bond lengths in the free HOPO ligand. In these eight-coordinate complexes, the average bond lengths between the lanthanide ion and the OPO oxygen atoms are in the range 2.364–2.392 Å. The difference in the average Ln–O bond lengths of complexes **1** and **4** is 0.028 Å, which is comparable with the difference in their ionic radii, Eu = 1.066 and Dy = 1.027 Å. These bond lengths are slightly shorter to that reported in nine-coordinate thorium complex of the 1-hydroxy-2-pyridinonate anion, $Th(OPO)_4\cdot H_2O$ (Th–O = 2.44 Å)[41] and significantly longer than those found in six-coordinate complexes of transition metals ($Fe(OPO)_3$, Fe–O = 2.008 Å; $Co(OPO)_3$, Co–O = 1.885 Å).[42] As one can see from Table 4, the shortening of the N–O (~0.05 Å) and N–C (~0.01 Å) bonds and the lengthening of the C–O (~0.05 Å) bonds indicates increased π-delocalisation over the O–C–N–O fragment upon complexation. The sum of the internal angles of the five-membered chelate ring are in the range 535.9–539.9° (Ln = Eu, Gd) and 539.2–539.4° (Ln = Tb, Dy). These angles are very close to 540, indicating that the five-membered rings are almost planar. The slight changes in the carbon–carbon bond lengths suggest increased delocalisation over the entire OPO ring.

OPO sensitized lanthanide luminescence

Since the OPO^- moiety binds to lanthanide(III) cations and absorbs in UV region with an appreciable molar absorptivity coefficient (λ = 316 nm, ε = 5000 M^{-1} cm^{-1}),[43] it may act as antenna group to photosensitize lanthanide luminescence. In fact, ligand sensitized lanthanide luminescence occurs when an organic ligand, which is coordinated to the metal ion, collects an UV excitation energy and channels it in a radiationless process through the triplet state to the resonant level of the lanthanide ion which emits its characteristic luminescence in the visible region.[20] We thus studied the luminescence behaviour of the europium(III), terbium(III) and dysprosium(III) complexes.

The time-resolved luminescence spectrum of the europium complex, recorded in the solid state at 295 K, is shown in Fig. 4. It consists in several bands related to the de-excitation from the lowest excited state, $^5D_0$, of the Eu^{3+} ion. The very intense band at 614 nm arises from the $^5D_0 \longrightarrow {}^7F_2$ transition. The four weak bands at 582, 596, 653 and 695 nm correspond to the transitions from the $^5D_0$ state to the $^7F_0$, $^7F_1$, $^7F_3$ and $^7F_4$ levels, respectively. The intensity repartition of these bands is different from the spectrum of $EuCl_3\cdot 6H_2O$, reflecting the substitution around the

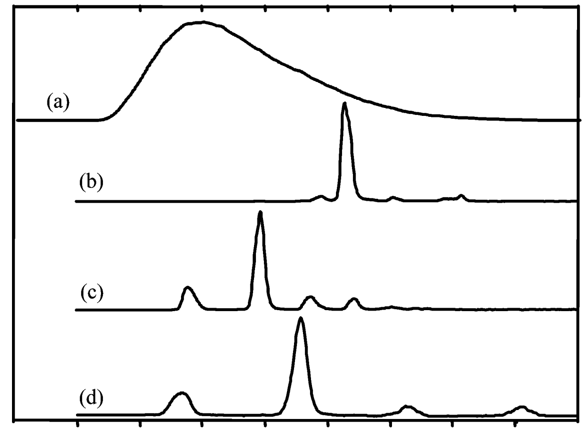

Fig. 4 Low-resolution time-resolved emission spectra of (a) Gd compound **2**, (b) Eu compound **1**, (c) Tb compound **3** and (d) Dy compound **4** in the solid state at 295 K (b), (c), (d) or at 77 K (a) (λ_{exc} = 320 nm).

Table 4 Average bond lengths (Å) in crystal structures of 1-hydroxy-2-pyridinone[18] and complexes **1**–**4**[a]

	Ln–O	N–O	C_a–O	N–C_a	C_c–C_d	Average (C_b–C_c/C_d–C_e)
HOPO		1.384	1.252	1.380	1.400	1.351
Eu	2.392	1.320	1.308	1.371	1.389	1.369
Gd	2.383	1.325	1.308	1.368	1.398	1.362
Tb[21]	2.368	1.332	1.290	1.367	1.392	1.362
Dy	2.364	1.338	1.295	1.374	1.397	1.370

[a] Lettering of atoms corresponds to ring position (see Scheme 1).

metal ion by coordinating atoms of the ligand of water molecules and chloride ions. Recording the intensity of the $^5D_0 \longrightarrow {}^7F_2$ transition as a function of excitation wavelength shows which absorption transitions lead to population of the Eu^{3+} emitting state. The resulting excitation spectrum displays only one broad band at 320 nm, which is assigned to an $S_0 \longrightarrow S_1$ absorption transition with the HOPO chromophore. No transition corresponding to the own Eu^{3+} absorption levels, especially the $^7F_0 \longrightarrow {}^5L_6$ and $^7F_0 \longrightarrow {}^5D_2$ transitions, located at 395 and 465 nm respectively, is observable in the excitation spectrum (Fig. 5). These results indicate that an indirect process, *i.e.* a ligand-to-metal inter-system energy transfer is the only photophysical pathway leading to observable luminescence in this sample. It has been established that some transitions of the Eu(III) emission show energy or intensity variations which depend upon the number, type or arrangement of ligating atoms in the first coordination sphere of the metal.[44] In Eu(III) complex **1**, the intensity ratio of the hypersensitive $^5D_0 \longrightarrow {}^7F_2$ transition and the magnetic dipole $^5D_0 \longrightarrow {}^7F_1$ transition is about 18, indicating that this complex has a structure with no imposed symmetry. As a matter of fact, complexes with a centrosymmetric coordination sphere have $^7F_2/^7F_1$ intensity ratios lower than 0.7, whereas an intensity ratio higher than 8 is indicative of a low-symmetry environment around the Eu(III) ion.[45] High-resolution laser luminescence experiments reveal for the $^5D_0 \longrightarrow {}^7F_0$ transition the existence of a unique component centred at 17215 cm^{-1} (full width at half height (fwhh) = 10 cm^{-1}) indicating the presence of a single Eu^{3+} coordination environment, in agreement with the results of X-ray single crystal analysis. Frey and Horrocks[46] showed that the energy of the $^5D_0 \longrightarrow {}^7F_0$ transition ($\tilde{\nu}_{obs}$) can be calculated from the equation $\tilde{\nu}_{obs} - \tilde{\nu}_0 = C_{CN}\, \Sigma_i n_i \delta_i$ where C_{CN} is a constant depending upon the Eu(III) coordination number (1.06 for CN = 8), n the number of coordinated atoms i, δ the energy shift parameter for atom i, and $\tilde{\nu}_0$ the energy of the $^5D_0 \longrightarrow {}^7F_0$ transition of the free ion (17374 cm^{-1}). By using this equation, a nephelauxetic shift parameter δ of -37.5 cm^{-1} can be calculated for a bidentate hydroxamate group. This high value is consistent with a strong M–L interaction and fairly matches the value of -36.4 cm^{-1} calculated for two unidentate carboxylate groups. Luminescence decay of the Eu(III) complex **1** was investigated by direct excitation of the ligand and by recording the intensity of the emitted light of the $^5D_0 \longrightarrow {}^7F_2$ transition. The decay profile fits a single-exponential law, confirming that all Eu^{3+} ions lie in the same average environment. The resulting lifetime of 0.22 ms at 295 K, reflects that an important deactivation process takes place. Since no water molecule is coordinated to the europium, the usual quenching effect of bound OH oscillators cannot be invoked in this case. A self-quenching process in a closely packed solid as reported for some europium complexes[47] is not operating, because similar lifetime values are observed in the solid state and in methanol solution[21] at 295 K. On the other hand, the five-fold increase in lifetime value upon going from 295 to 77 K indicates that an important role of the Eu^{3+} emitting state is played by a thermally activated radiationless decay path. For Eu^{3+} complexes, it is well established that an important quenching mechanism involves the population of ligand-to-metal charge transfer (LMCT) excited states from the $^5D_0$ Eu^{3+} emitting state, followed by efficient non-radiative decay to the ground state.[20] A low-lying LMCT excited states involving the carbonyl group of the four OPO^- ligands may account for the weak luminescence observed for complex **1**. Although LMCT transition could not be evidenced in the excitation spectrum, due to the presence of more intense ligand centred band, the influence of LMCT excited states on the $^5D_0$ luminescence quenching process in complexes containing amide carbonyl functions is well documented.[48]

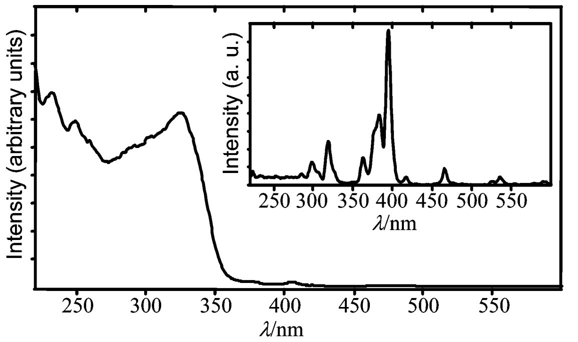

Fig. 5 Excitation spectrum of Eu compound **1** in the solid state at 295 K (λ_{em} = 614 nm). The inset in this figure is the excitation spectrum of $EuCl_3 \cdot 6H_2O$ in the solid state at 295 K (λ_{em} = 614 nm).

No ligand-to-metal energy transfer and the consequent MC luminescence are observed for the Gd(III) complex. This is an expected result since the lowest excited state ($^6P_{7/2}$) of the Gd^{3+} ion lies above 31000 cm^{-1},[49] *i.e.* at higher energy than the emitting excited states of the free ligand. Upon UV excitation at 77 K, the emission spectrum of the Gd(III) complex **2** shows a broad band extending from 400 to 750 nm, with a maximum at 499 nm and lifetime of 5.7 ms. It therefore originates from the ligand $^3\pi\pi^*$ state. Unfortunately, this emission band is not vibrationally structured (Fig. 4), and consequently it is not possible to determine the $^3S_1^*$ triplet level by considering the lowest emission wavelength (0–0 transition). However, we can note that for the Eu, Tb and Dy complexes **1**, **3**, **4**, the emission from the $^3\pi\pi^*$ state is completely quenched, pointing to an efficient ligand-to-metal energy-transfer process in these complexes.

Photoexcitation of the OPO antenna at 320 nm in the Tb(III) complex **3** gives an entirely typical Tb(III) emission spectrum containing the expected sequence of $^5D_4 \longrightarrow {}^7F_j$ transitions, with j = 6–2 components being visible (Fig. 4). The spectrum is dominated by the $^5D_4 \longrightarrow {}^7F_5$ transition, (64% of the total emission) peaking at 547 nm, which gives an intense green luminescence output for the solid sample. The spectral distribution differs from that of $TbCl_3 \cdot 6H_2O$, but this does not provide a basis for an evaluation of the inner coordination of the Tb(III) ion, as in the case of Eu(III) spectra.[44] Despite the presence of two water molecules in the Tb(III) coordination sphere, which provides an effective non-radiative de-excitation pathway, the terbium complex displays higher luminescence intensity and lifetime (0.60 ms at 295 K) than those measured for the europium complex **1**. The intrinsic luminescence quantum yield of the lanthanide ion (ϕ^{lum}) can be calculated from the observed emission lifetime τ_{obs} and pure radiative lifetime τ_R, since $\phi^{lum} = \tau_{obs}/\tau_R$. According to Klink *et al.*,[50] typical values of the natural lifetime τ_R of Eu^{3+} and Tb^{3+} are 3 and 4 ms, respectively. Using these values, the intrinsic luminescence efficiency at the terbium centre in $[Tb(OPO)_3(H_2O)_2]\cdot H_2O$ is two times higher than for the Eu^{3+} ion in $Na[Eu(OPO)_4]\cdot 4.5H_2O$ (15 *vs* 7.3%). Moreover, the lifetime of the $^5D_4$(Tb) level increases only marginally (7%) upon decreasing the temperature to 77 K. Thermal energy back transfer, which is the principal quenching mechanism of the luminescent excited state of Tb(III) complexes, seems therefore to be of minor importance in complex **3**. Looking at the energy of the ligand triplet states in 42 terbium complexes, Latva *et al.*[51] conclude that the energy back transfer is observed when the energy difference between the $^5D_4$ level of Tb(III) (20400 cm^{-1}) and the lowest triplet state energy level of the ligand is less than about 1850 cm^{-1}. This indicates that the energy of the lowest triplet state of the OPO^- ligand is above 22250 cm^{-1}.

The $^4F_{9/2}$ acceptor level of the Dy^{3+} ion lies around 21000 cm^{-1}, slightly higher in energy than the $^5D_4$(Tb) level, so a sizeable $OPO^- \longrightarrow$ Dy energy transfer is expected. Upon excitation of the Dy complex at 320 nm, the typical luminescence bands are observed corresponding to the $^4F_{9/2} \longrightarrow {}^6H_j$ transitions. This complex shows four emission bands in the visible region, two strong bands at 484 and 579 nm and two weaker bands at 663 and 755 nm. The lifetime of the emission band at 579 nm was determined to be 20 μs, which is within the general range of lifetimes for Dy(III) ions.[52] This shorter emission lifetime compared to the Tb^{3+} complex, although these two complexes are isostructural, is the effect of the smaller energy gap between the lowest luminescent state, $^4F_{9/2}$, and the ground state, $^4F_{3/2}$, of Dy^{3+} ion ($\Delta E_{\mathrm{Dy}^{3+}}$ = 7850 cm^{-1} compared to $\Delta E_{\mathrm{Tb}^{3+}}$ = 14200 cm^{-1}).[49] This relatively small energy gap of Dy^{3+} is easily matched by a lower overtone of an O–H vibration mode, leading to a very effective quenching of the $^4F_{9/2}$ excited state and henceforth a weak emission.

Conclusion

In conclusion, this study gives a new light on the interaction between lanthanide(III) ions and hydroxamate ligands. The synthesis and crystal structures of novel Eu, Gd, Tb and Dy compounds derived from the 1-hydroxy-2-pyridinone ligand demonstrate that (a) the HOPO ligand can chelate a Ln(III) ion in a bidentate coordination through the oxygen atoms and shows a rich variety of coordination modes, (b) these complexes are air/moisture stable, (c) they have the same coordination number (8), but their ligand : metal stoichiometry are not equivalent across the series. This last result highlights the caution that one must take in extending the results obtained for one complex to the other lanthanides. Our study further demonstrates that the HOPO ligand possesses a UV absorption band suitable for pumping Ln^{3+} luminescence. While the HOPO ligand is a poor sensitizer for Eu(III) ion, which may have some connection with the presence of LMCT excited states, it transfers energy efficiently to Tb(III) without the usual energy back transfer quenching process. The stability and bright luminescence of compound **3** reveal the attractiveness of HOPO moieties as potentially new types of building blocks for devices with long-lived photoluminescence.

Acknowledgements

The authors thank Dr J. Dexpert-Ghys at the Centre National de la Recherche Scientifique for the measurement of high-resolution luminescence spectra and helpful discussions.

References

1 *Rare Earths*, ed. R. Saez Puche and P. Caro, Editorial Complutense, Madrid, 1998.

2 P. Caravan, J. J. Ellison, T. J. McMurry and R. B. Lauffer, *Chem. Rev.*, 1999, **99**, 2293–2352; S. Aime, M. Botta, M. Fasano and E. Terreno, *Chem. Soc. Rev.*, 1998, **27**, 19–29.

3 D. J. Bornhop, D. S. Hubbard, M. P. Houlne, C. Adair, G. E. Kiefer, B. C. Pence and D. L. Morgan, *Anal. Chem.*, 1999, **71**, 2607–2615; G. Ferro-Flores, F. D. M. Ramírez, J. I. Tendilla, G. Pimentel-González, C. A. Murphy, L. Meléndez-Alafort, J. A. Ascencio and B. Y. Croft, *Bioconjugate Chem.*, 1999, **10**, 726–734; G. R. Boniface, M. E. Izard, K. Z. Walker, D. R. McKay, P. J. Sorby, J. H. Turner and J. G. Morris, *J. Nucl. Med.*, 1989, **30**, 683–691.

4 D. Nayak and S. Lahiri, *J. Radioanal. Nucl. Chem.*, 1999, **242**, 423–432; J. L. Sessler, V. Kral, M. C. Hoehner, K. O. A. Chin and R. M. Davila, *Pure Appl. Chem.*, 1996, **68**, 1291–1295; J. L. Sessler, W. C. Dow, D. O'Connor, A. Harriman, G. Hemmi, T. D. Mody, R. A. Miller, F. Qing, S. Springs, K. Woodburn and S. W. Young, *J. Alloys Compd*, 1997, **249**, 146–152; N. V. Jarvis, J. M. Wagener and G. E. Jackson, *J. Chem. Soc., Dalton Trans.*, 1995, 1411–1415.

5 A. J. Kolb, J. W. Burke and G. Mathis, in *High Throughput Screening: The Discovery of Bioactive Substances*, ed. J. P. Devlin, M. Dekker, New York, 1997, ch. 19, pp. 345–360; I. Hemmilä, T. Stahlberg and P. Mottram, in *Bioanalytical Applications of Labeling Technologies*, ed. Wallac Oy, Turku, 2nd edn., 1995.

6 J. Hovinen and H. Hakala, *Org. Lett.*, 2001, **3**, 2473–2476; H. Takalo, V.-M. Mukkala, L. Meriö, J.-C. Rodriguez-Ubis, R. Sedano, O. Juanes and E. Brunet, *Helv. Chim. Acta*, 1997, **80**, 372–387.

7 M. H. V. Werts, R. H. Woudenberg, P. G. Emmerink, R. van Gassel, J. W. Hofstraat and J. W. Verhoeven, *Angew. Chem., Int. Ed.*, 2000, **39**, 4542–4544; A. Beeby, R. S. Dickins, S. Faulkner, D. Parker and J. A. G. Williams, *Chem. Commun.*, 1997, 1401–1402.

8 A. I. Voloshin, N. M. Shavaleev and V. P. Kazakov, *J. Photochem. Photobiol., A*, 2000, **134**, 111–117 and references therein.

9 S. Liu and D. S. Edwards, *Bioconjugate Chem.*, 2001, **12**, 7–34.

10 B. Chatterjee, *Coord. Chem. Rev.*, 1978, **26**, 281–303.

11 A.-M. Albrecht-Gary and A. L. Crumbliss, in *Metal Ions in Biological Systems*, ed. A. Sigel and H. Sigel, M. Dekker, New York, 1998, vol. 35, ch. 7, pp. 239–328.

12 I. May, R. J. Taylor, I. S. Denniss, G. Brown, A. L. Wallwork, N. J. Hill, J. M. Rawson and R. Less, *J. Alloys Compd*, 1998, **275–277**, 769–772; L. Dasaradhi, P. C. Stark, V. J. Huber, P. H. Smith, G. D. Jarvinen and A. S. Gopalan, *J. Chem. Soc., Perkin Trans. 2*, 1997, 1187–1192; T. Nagasaki, S. Shinkai and T. Matsuda, *J. Chem. Soc., Perkin Trans. 1*, 1990, 2617–2618.

13 A. Evers, R. D. Hancock, A. E. Martell and R. J. Motekaitis, *Inorg. Chem.*, 1989, **28**, 2189–2195.

14 B. Kurzak, H. Kozlowski and E. Farkas, *Coord. Chem. Rev.*, 1992, **114**, 169–200.

15 E. Galdecka, Z. Galdecki, P. Gawryszewska and J. Legendziewicz, *New J. Chem.*, 1998, **22**, 941–945.

16 C. Galaup, J. Azéma, P. Tisnès, C. Picard, P. Ramos, O. Juanes, E. Brunet and J.-C. Rodríguez-Ubis, *Helv. Chim. Acta*, 2002, **85**, 1613–1625; C. Galaup, J. M. Couchet, C. Picard and P. Tisnès, *Tetrahedron Lett.*, 2001, **42**, 6275–6278; C. Galaup, M.-C. Carrié, P. Tisnès and C. Picard, *Eur. J. Org. Chem.*, 2001, 2165–2175; J. Azéma, C. Galaup, C. Picard, P. Tisnès, P. Ramos, O. Juanes, J.-C. Rodriguez-Ubis and E. Brunet, *Tetrahedron*, 2000, **56**, 2673–2681; C. Galaup, C. Picard, B. Cathala, L. Cazaux, P. Tisnès, H. Autiero and D. Aspe, *Helv. Chim. Acta*, 1999, **82**, 543–560.

17 J. N. Gardner and A. R. Katritzky, *J. Chem. Soc.*, 1957, 4375–4387 and references therein.

18 P. Ballesteros, R. M. Claramunt, T. Canada, C. Foces-Foces, F. Hernandez Cano, J. Elguero and A. Fruchier, *J. Chem. Soc., Perkin Trans. 2*, 1990, 1215–1219.

19 S. I. Weissman, *J. Chem. Phys.*, 1942, **10**, 214–217.

20 N. Sabbatini, M. Guardigli and J.-M. Lehn, *Coord. Chem. Rev.*, 1993, **123**, 201–228.

21 C. Tedeschi, C. Picard, J. Azéma, B. Donnadieu and P. Tisnès, *New J. Chem.*, 2000, **24**, 735–737.

22 E. Shaw, *J. Am. Chem. Soc.*, 1949, **71**, 67–70.

23 G. M. Sheldrick, *Acta Crystallogr., Sect. A*, 1990, **46**, 467–473.

24 G. M. Sheldrick, SHELXL-97, Program for Crystal Structure Refinement, University of Göttingen,1997.

25 Y. K. Agrawal and J. P. Shukla, *J. Indian Chem. Soc.*, 1974, **53**, 373.

26 K. Bhatt and Y. K. Agrawal, *Synth. Inorg. Met.-Org. Chem.*, 1972, **2**, 175–179.

27 M. E. Mesquita, G. F. de Sa, M. A. B. Lopes and O. L. Malta, *J. Chem. Res. (S)*, 1996, 120–121.

28 D. A. Brown, D. McKeith and W. K. Glass, *Inorg. Chim. Acta*, 1979, **35**, 57–60; A. Das, F. Basuli, S.-M. Peng and S. Bhattacharya, *Inorg. Chem.*, 2002, **41**, 440–443.

29 A. E. Landers and D. J. Phillips, *Inorg. Chim. Acta*, 1981, **51**, 109–115.

30 A. R. Katritzky and R. A. Jones, *J. Chem. Soc.*, 1960, 2947–2953.
31 G. Hopfgartner, C. Piguet and J. D. Henion, *J. Am. Soc. Mass Spectrom.*, 1994, **5**, 748–756.
32 J. M. Curtis, P. J. Derrick, A. Schnell, E. Constantin, R. T. Gallagher and J. R. Chapman, *Inorg. Chim. Acta*, 1992, **201**, 197–201.
33 D. M. L. Goodgame, S. P. W. Hill and D. J. Williams, *Inorg. Chim. Acta*, 1998, **272**, 131–140.
34 R. D. Shannon, *Acta Crystallogr., Sect. A*, 1976, **32**, 751–767.
35 G. R. Chopin, in *Lanthanide Probes in Life, Chemical, and Earth Sciences. Theory and Practice*, ed. J.-C. Bünzli and G. R. Choppin, Elsevier, 1989, ch. 1, pp. 1–41.
36 A. Dobosz, N. M. Dudarenko, I. O. Fritsky, T. Glowiak, A. Karaczyn, H. Kozlowski, T. Y. Sliva and J. Swiatek-Kozlowska, *J. Chem. Soc., Dalton Trans.*, 1999, 743–749.
37 J.-K. Tang, Y.-Z. Li, Q.-L. Wang, E.-Q. Gao, D.-Z. Liao, Z.-H. Jiang, S.-P. Yan, P. Cheng, L.-F. Wang and G.-L. Wang, *Inorg. Chem.*, 2002, **41**, 2188–2192.
38 J. L. kropp and M. W. Windsor, *J. Chem. Phys.*, 1965, **42**, 1599–1608; Y. Haas and G. Stein, *J. Phys. Chem.*, 1971, **75**, 3677–3681.
39 A. S. Gajadhar-Plummer, I. A. Kahwa, A. J. P. White and D. J. Williams, *Inorg. Chem.*, 1999, **38**, 1745–1753; P. A. Brayshaw, J.-C. G. Bünzli, P. Froidevaux, J. M. Harrowfield, Y. Kim and A. N. Sobolev, *Inorg. Chem.*, 1995, **34**, 2068–2076.
40 S. R. Drake, A. Lyons, D. J. Otway and D. J. Williams, *Inorg. Chem.*, 1994, **33**, 1230–1233.
41 P. E. Riley, K. Abu-Dari and K. N. Raymond, *Inorg. Chem.*, 1983, **22**, 3940–3944.
42 R. C. Scarrow, P. E. Riley, K. Abu-Dari, D. L. White and K. N. Raymond, *Inorg. Chem.*, 1985, **24**, 954–967.
43 B. M. Aveline, I. E. Kochevar and R. W. Redmond, *J. Am. Chem. Soc.*, 1996, **118**, 10124–10133.
44 F. S. Richardson, *Chem. Rev.*, 1982, **82**, 541–552.
45 A. F. Kirby, D. Foster and F. S. Richardson, *Chem. Phys. Lett.*, 1983, **95**, 507–512; A. F. Kirby and F. S. Richardson, *J. Phys. Chem.*, 1983, **87**, 2544–2556.
46 S. T. Frey and W. De W. Horrocks Jr., *Inorg. Chim. Acta*, 1995, **229**, 383–390.
47 G. Muller, B. Schmidt, J. Jiricek, G. Hopfgartner, J. P. Riehl, J.-C. G. Bünzli and C. Piguet, *J. Chem. Soc., Dalton Trans.*, 2001, 2655–2662.
48 F. De M. Ramírez, L. Charbonnière, G. Muller, R. Scopelliti and J.-C. G. Bünzli, *J. Chem. Soc., Dalton Trans.*, 2001, 3205–3213; H. Matsumoto and S. Shinkai, *Chem. Lett.*, 1994, 901–904; N. Sabbatini, M. Guardigli, A. Mecati, V. Balzani, R. Ungaro, E. Ghidini, A. Casnati and A. Pochini, *J. Chem. Soc., Chem. Commun.*, 1990, 878–879.
49 G. Stein and E. Würzberg, *J. Chem. Phys.*, 1975, **62**, 208–213.
50 S. I. Klink, L. Grave, D. N. Reinhoudt, F. C. J. M. van Veggel, M. H. V. Werts, F. A. J. Geurts and J. W. Hofstraat, *J. Phys. Chem. A*, 2000, **104**, 5457–5468.
51 M. Latva, H. Takalo, V.-M. Mukkala, C. Matachescu, J.-C. Rodriguez-Ubis and J. Kankare, *J. Lumin.*, 1997, **75**, 149–169.
52 E. Brunet, O. Juanes, R. Sedano and J.-C. Rodriguez-Ubis, *Photochem. Photobiol. Sci.*, 2002, **1**, 613–618.